CARTILAGE
2021, Vol. 13(Suppl 2) 1742S–1754S

DOI: 10.1177/19476035211060508
journals.sagepub.com/home/CAR
SAGE

Methodology to Quantify Collagen Subtypes and Crosslinks: Application in Minipig Cartilages

Benjamin J. Bielajew[1], Jerry C. Hu[1], and Kyriacos A. Athanasiou[1]

Abstract

Introduction. This study develops assays to quantify collagen subtypes and crosslinks with liquid chromatography-mass spectrometry (LC-MS) and characterizes the cartilages in the Yucatan minipig. *Methods.* For collagen subtyping, liquid chromatography-tandem mass spectrometry (LC-MS/MS) analysis was performed on tissues digested in trypsin. For collagen crosslinks, LC-MS analysis was performed on hydrolysates. Samples were also examined histologically and with bottom-up proteomics. Ten cartilages (femoral condyle, femoral head, facet joint, floating rib, true rib, auricular cartilage, annulus fibrosus, 2 meniscus locations, and temporomandibular joint disc) were analyzed. *Results.* The collagen subtyping assay quantified collagen types I and II. The collagen crosslinks assay quantified mature and immature crosslinks. Collagen subtyping revealed that collagen type I predominates in fibrocartilages and collagen type II in hyaline cartilages, as expected. Elastic cartilage and fibrocartilages had more mature collagen crosslink profiles than hyaline cartilages. Bottom-up proteomics revealed a spectrum of ratios between collagen types I and II, and quantified 42 proteins, including 24 collagen alpha-chains and 12 minor collagen types. *Discussion.* The novel assays developed in this work are sensitive, inexpensive, and use a low operator time relative to other collagen analysis methods. Unlike the current collagen assays, these assays quantify collagen subtypes and crosslinks without an antibody-based approach or lengthy chromatography. They apply to any collagenous tissue, with broad applications in tissue characterization and tissue engineering. For example, a novel finding of this work was the presence of a large quantity of collagen type III in the white-white knee meniscus and a spectrum of hyaline and fibrous cartilages.

Keywords

collagen, collagen subtype, mass spectrometry, collagen crosslinks, cartilage, fibrocartilage

Introduction

Collagen is the most abundant protein in the mammalian body and is the foundation of the extracellular matrix (ECM) of connective tissues.[1] Collagen is better described as a superfamily of proteins consisting of 28 currently discovered subtypes, each of which is a trimer consisting of 3 alpha-chains that associate into supercoiled triple helices.[2] The main fibrillar collagen subtypes, collagen types I and II, make up a large majority of collagens found in different tissues all over the body.[1] A primary barrier to determining the collagen composition of biological tissues is that high-throughput and low-cost methods for collagen subtype quantification remain a major challenge.[1] The traditional method of collagen quantification, the hydroxyproline assay, does not discriminate among collagen subtypes.[3] Other methods, such as enzyme-linked immunosorbent assay (ELISA), can be prohibitively expensive or unavailable depending on the animal species or collagen subtype.[1] Some imaging methods, such as immunohistochemistry, can be used to visualize different collagen subtypes, but these are nonquantitative.[1]

In this work, we introduce a liquid chromatography-tandem mass spectrometry (LC-MS/MS) assay that uses multiple reaction monitoring[4] to quantify collagen types I and II. This assay is inexpensive compared with antibody-based methods and applicable to collagenous tissues from human, bovine, porcine, and murine sources. Enzymatic collagen crosslinks, such as the mature trivalent crosslink pyridinoline (PYR) and the immature divalent crosslink dihydroxylysinonorleucine

[1]Department of Biomedical Engineering, University of California, Irvine, Irvine, CA, USA

Corresponding Author:
Kyriacos A. Athanasiou, Department of Biomedical Engineering, University of California, Irvine, Irvine, CA 92697, USA.
Email: athens@uci.edu

(DHLNL), play important roles in the mechanical properties of collagenous tissues.[5,6] Recent work has introduced the use of diamond hydride chromatography for collagen crosslink quantification,[7] and, in this experiment, this chromatography method is used on an LC-MS with high sensitivity and specificity. As a demonstration of these 2 novel assays, 10 cartilages of the Yucatan minipig are analyzed. This animal model was selected because it is a well-recognized model for cartilage repair studies.[8,9]

Cartilages are classified into 1 of 3 categories: hyaline cartilage, fibrocartilage, and elastic cartilage, based on the composition of the tissue's ECM. Traditionally, cartilages are classified by the types of fibrillar proteins within the tissue. Hyaline cartilage, found on the ends of bones (articular cartilage) and in the ribs, nose, and trachea, is mostly collagen type II by dry weight (DW).[10] Fibrocartilage, found in the knee meniscus, temporomandibular joint (TMJ), and annulus fibrosus, has an ECM that contains mostly collagen type I by DW.[11] Elastic cartilage, found in the auricle of the ear and in the epiglottis, has an ECM that contains both collagen types I and II, as well as a substantial portion of elastin.[12]

Previous tissue engineering studies have shown that it is possible to engineer a spectrum of hyaline and fibrous cartilages, based on the ratio of collagen types I and II[13], that is, more hyaline cartilage having more collagen type II and less collagen type I, and more fibrous cartilage having more collagen type I and less collagen type II. While there has been evidence of higher collagen type II in the white-white portion of the knee meniscus compared with the red-red meniscus,[14] it is not known whether a wide spectrum of collagen ratios exist in native cartilages. Prior work has shown that femoral condylar cartilage contains higher PYR crosslinks compared with knee meniscus in the immature knee joint,[5] but it is unknown whether this trend holds true for other cartilages or for mature joints.

The objectives of this work are to develop high-throughput LC-MS assays to analyze collagen subtypes and crosslinks, to use these assays to characterize 10 cartilages of the Yucatan minipig, and to use bottom-up proteomics to quantitatively characterize the proteome of these minipig cartilages. The hypotheses of this work are that: (1) the LC-MS/MS collagen subtyping assay can quantify marker peptides of collagen types I and II in a specific and sensitive manner, and (2) the LC-MS collagen crosslinks assay can quantify PYR, DHLNL, and hydroxyproline. Using minipig cartilages as examples, it is expected that: (1) the novel collagen subtyping assay will show a majority of collagen type I in fibrocartilages and a majority of collagen type II in hyaline cartilages, (2) the collagen crosslinks assay will show different crosslink ratios in hyaline cartilages than fibrocartilages, and (3) bottom-up proteomics will reveal different ratios of collagen types I and II in different cartilages within the traditional hyaline and fibrous classifications, revealing a spectrum of cartilage tissues.

Methods

LC-MS/MS for Collagen Subtype Quantification

A Waters ACQUITY UPLC I-Class core system coupled to a Waters Quattro Premier XE triple quadrupole mass spectrometer was used for the collagen subtype LC-MS/MS assay. For all liquid chromatography in this study, solvent A was 0.1% (v/v) formic acid in water and solvent B was 0.1% (v/v) formic acid in acetonitrile. Liquid chromatography gradient settings were as follows: initial, 3% B; 2 minutes, 40% B; 3 minutes, 97% B; 4 minutes, 3% B; 5 minutes, 3% B; total run time, 5 minutes. An ACQUITY UPLC BEH C18 column was used with a flow rate of 300 µl/min for reverse-phase separation. Target peptides of collagen were selected under the following criteria: susceptible to digestion from trypsin; not found in any other protein aside from 1 specific collagen subtype; found in human, bovine, porcine, and murine tissues; and mass between 800 and 1800 Da. Briefly, PeptideRank was used for *in silico* prediction of tryptic peptides for collagen subtypes with the best ionization characteristics.[15] Peptides were checked with NCBI BLASTp to ensure uniqueness and identical sequence across human, bovine, porcine, and murine proteomes. The set of determined peptides is summarized in **Table 1.** After a peptide was selected, a custom synthesis of the peptide standard was ordered from GenScript. Multiple reaction monitoring (MRM) methods were developed by diluting peptide standards to 10 µg/ml in solvent A and then optimizing cone voltage (CV) and collision energy (CE) to ±1 V on repeated 5 µl injections. Standard curves were prepared by 3x serial dilution of a 10 µg/ml mix of the col1α1 and col2α1 peptide standards. Limit of detection (LOD) and limit of quantification (LOQ) were calculated based on a signal-to-noise ratio of 3 (LOD) or 10 (LOQ), calculated based on injections of the lowest concentration standard.

Quantification of Collagen Crosslinks and Hydroxyproline

Liquid chromatography gradient settings were as follows: initial, 90% B; 1 minute, 90% B; 2 minutes, 20% B; 4 minutes, 20% B; 5 minutes, 90% B; 10 minutes, 90% B; total run time, 10 minutes. A Cogent Diamond Hydride 2.o HPLC column was used with a flow rate of 400 µl/min for aqueous normal phase separation, coupled to a Waters ACQUITY QDa mass spectrometer. PYR standard was ordered from BOC Sciences, DHLNL standard was ordered from Santa Cruz Biotechnology, and hydroxyproline (OHP) and pyridoxine (PDX) standards were ordered from Sigma Aldrich. Quantification methods were developed by diluting PYR, DHLNL, OHP, and PDX standards to 1 µg/ml in solvent A and then optimizing CV to ±1 V on repeated 5 µl injections. Standard curves were prepared by 3x serial dilution of a 1 µg/ml mix of PYR, DHLNL, and PDX and 10

Table 1. Mass Spectrometry Settings for Target Analytes.

Analyte	Peptide Sequence	Mass (Da)	Parent m/z	Daughter m/z	CV (V)	CE (V)
Col1α1	GVQGP**P**GPAGPR	1104.58	553.93	668.2	27	30
Col2α1	GIVGL**P**GQR	911.53	457.3	474.46	21	13
Hydroxyproline	n/a	131.13	132.17	n/a	6	n/a
PYR	n/a	428.19	215.21	n/a	6	n/a
DHLNL	n/a	307.34	308.30	n/a	6	n/a
Pyridoxine	n/a	169.18	170.08	n/a	6	n/a

Bold **P** represents hydroxyproline.
CV = cone voltage; CE = collision energy; PYR = pyridinoline; DHLNL = dihydroxylysinonorleucine.

μg/ml of OHP. PDX was used as an internal standard. LOD and LOQ were calculated as described above.

Bottom-up Proteomics

For all bottom-up proteomics samples, the same peptide digest used for the collagen I and II LC-MS/MS assay was used. For each tissue, digests from all 7 animals were combined into 1 representative sample. The peptide digests were subjected to LC-MS/MS analysis using a Thermo Fischer Scientific UltiMate 3000 RSLC system coupled on-line to a Thermo Fischer Scientific Orbitrap Fusion Lumos mass spectrometer. Liquid chromatography gradient was as follows: 4% to 25% solvent B over 57 minutes. A 50 cm × 75 μm I.D. Acclaim® PepMap RSLC column was used at a flow rate of 300 nl/min for reverse-phase separation. Each cycle consisted of 1 full Fourier transform scan mass spectrum (375-1500 m/z, resolution of 60,000 at m/z 400) followed by 15 data-dependent MS/MS acquired in the linear ion trap with collision-induced dissociation with normalized CE of 25%. Target ions already selected for MS/MS were dynamically excluded for 30 seconds. Identification and label-free quantification were carried out using MaxQuant, as previously described.[16] Briefly, raw files were searched using MaxQuant (v. 1.6.0.16) against a FASTA containing the *sus scrofa* proteome obtained from the SwissProt open-source database (version from December 2020) along with *sus scrofa* collagen proteins from TrEMBL. The first search peptide tolerance was set to 20 ppm, with main search peptide tolerance set to 4.5 ppm. The protein, peptide, and peptide spectrum match level false discovery rates were all 1% as determined by a target-decoy approach. For quantification, intensities were determined as the full peak volume over the retention time profile. The degree of uniqueness required for peptides to be included in quantification was "Unique plus razor peptides." The resulting label-free quantification (LFQ) values calculated through MaxQuant were used for comparing protein relative abundance among different samples. The proteomics data have been deposited to the ProteomeXchange Consortium via the PRIDE partner repository with the data set identifier PXD025482.

Data Analysis and Statistical Analysis

For collagen types I and II and for collagen crosslinks, MassLynx v4.1 software with QuanLynx was used to calculate area-under-curve measurements for all MRM peaks for interpolation into the standard curve. The resulting ng/ml result was multiplied by the sample volume and appropriate dilution factor to quantify the analyte quantity in the sample. Any analyte quantity below the LOQ was set to zero. For crosslinks, the resulting mass of each crosslink was normalized to DW or the amount of hydroxyproline in the hydrolysate. For peptides, the peptide mass was converted to protein mass. For collagen type II, the peptide mass (M_{pep}) is multiplied by the mass ratio of the alpha-chain to peptide (k) to calculate the mass of collagen type II in the digest (M_{Col2}):

$$M_{Col2} = kM_{pep}$$

For collagen type I, protein mass is calculated based on the quantification of the col1α1 peptide; because collagen type I is a heterotrimer which has 2 col1α1 chains and 1 col1α2 chain, the mass may be calculated, assuming the molar ratio of col1α1 to col1α2 to be 2:1. Here, k is the mass ratio of a col2α1 molecule to the col2α1 target peptide, and A is the molar ratio of 1 col1α2 molecule to 2 col1α1 molecules as calculated by their amino acid sequences and posttranslational modifications:

$$\begin{aligned} M_{Col1} = M_{Col1\alpha1} + M_{Col1\alpha2} &= (1+A)M_{Col1\alpha1} \\ &= (1+A)(kM_{pep}) \end{aligned}$$

For collagen type II, $k = 105.09$. For collagen type I, $k = 86.01$ and $A = 0.49$. Molecular weights of the collagen proteins were calculated after cleavage of the N-terminal propeptides. Protein masses were normalized to sample DW.

Statistical analysis was performed in JMP Pro 14. *Post hoc* Tukey tests were used after performing 1-way analyses

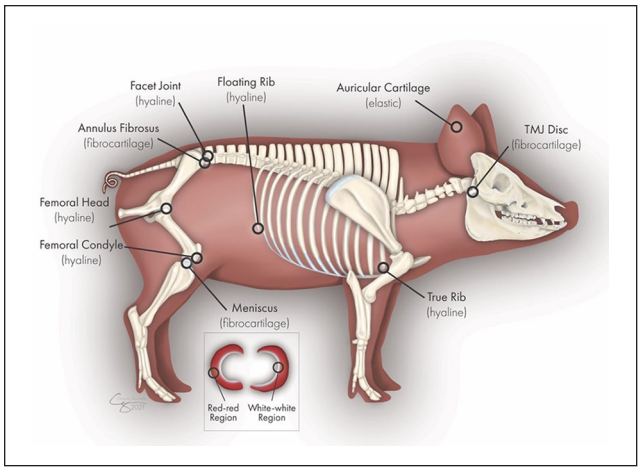

Figure 1. The locations of the different cartilages harvested from the Yucatan minipig. Illustration by Chrisoula Skouritakis. TMJ = temporomandibular joint.

of variance (ANOVAs). Statistical significance ($P < 0.05$) is indicated with a connecting-letters report on all bar graphs; bars not sharing the same letter are significantly different from each other. All graphs were generated in GraphPad Prism 8.

Sample Preparation

Ten cartilage tissues from the Yucatan minipig were analyzed: knee meniscus (both red-red portion and white-white portion separately), TMJ disc (center region), annulus fibrosus of the intervertebral disc (L5/S1 or L6/S1 joint), auricular (ear) cartilage, femoral head cartilage, femoral condyle cartilage, costal cartilages of the true rib (rib 1) and floating rib (rib 14), and facet joint cartilage (**Fig. 1**). Cartilage pieces were excised from $N = 7$ skeletally mature (5-6 month old) Yucatan minipigs which were previously culled for reasons unrelated to this study. For histological analysis, 5 mm biopsies from 3 representative pieces of each cartilage type were fixed in formalin, embedded in paraffin, sectioned to 5 µm thickness, and stained with hematoxylin and eosin (H&E) or picrosirius red (PR) as previously described.[17] Two 1.5-mm biopsy samples (0.5-1 mg wet weight) from each cartilage piece were washed in ultrapure water, dabbed dry, weighed for wet weight, lyophilized, and weighed again for DW. One biopsy sample was used for the collagen subtyping assay and bottom-up proteomics, and the other was used for the crosslinks assay.

For collagen subtyping and bottom-up proteomics, samples were washed twice in 10 mM ammonium citrate and twice in 50 mM ammonium bicarbonate, and then mass spectrometry–grade trypsin was added in a 1:20 (w/w) ratio of trypsin to sample DW, and samples were digested at 65°C in 200 µl of 50 mM ammonium bicarbonate. After digestion, samples were filtered through 100 kDa molecular weight cut-off centrifugal filters and diluted 1:1 in 0.1% formic acid, yielding a transparent, colorless peptide digest solution. For the crosslinks assay, biopsy samples were submerged in 1 mM NaOH containing $NaBH_4$ (1% weight to sample weight) for 2 hours at room temperature, washed overnight in ultrapure water, and then hydrolyzed in 6N HCl at 105°C for 18 hours in a heat block. HCl was evaporated, and samples were resuspended in 400 µl of 0.1% formic acid, then filtered through 100 kDa molecular weight cut-off centrifugal filters, and diluted 20:1 in 0.1% formic acid, yielding a transparent, colorless hydrolysate.

Results

LC-MS Assays for Collagen Subtypes and Crosslinks

The determined parameters required for running the LC-MS/MS assays for collagen subtype and crosslink quantification are displayed in **Table 1**. The collagen subtyping assay quantified col1α1 and col2α1 marker peptides in biological tissues in a 5-minute chromatography gradient, and the collagen crosslinks assay quantified PYR, DHLNL, and hydroxyproline in a 10-minute chromatography gradient. For the col1α1 marker peptide, the LOD was 40.7 ng/ml and the LOQ was 135.7 ng/ml. For the col2α1 marker peptide, the LOD was 9.5 ng/ml and the LOQ was 31.9 ng/ml. For a 200-µg DW sample, these LOQs correspond to a quantifiable amount of collagen at approximately 3.5% collagen type I/DW and 0.7% collagen type II/DW. Both marker peptides' standard curves yielded a strong goodness of fit ($R^2 > 0.99$). To translate the assay result of peptide ng/ml to a protein/DW, complete digestion of the tissue is necessary. The technique of single-step high-temperature trypsin digestion at 65°C rather than the standard 37°C yielded peptide digests that were transparent, colorless, and absent of any undigested tissue (with the exception of mineralized tissues), indicating that digestion was complete. For collagen crosslinks, the LOD and LOQ of hydroxyproline were 2.7 and 8.9 ng/ml, LOD and LOQ of PYR were 6.5 and 21.5 ng/ml, and LOD and LOQ of DHLNL were 0.6 and 2.0 ng/ml, respectively. This degree of sensitivity was sufficient to quantify PYR, DHLNL, and hydroxyproline in all tested tissues.

Collagens in Minipig Cartilages

Collagen types I and II were quantified in 10 tissues via LC-MS/MS high-throughput quantification (**Fig. 2A and B**); data are presented as collagen mass per DW. For collagen type I, the fibrocartilages had the highest amount per DW. TMJ disc had the highest content out of the fibrocartilages, at 85.1% ± 4.0% per DW. All hyaline cartilages (true rib,

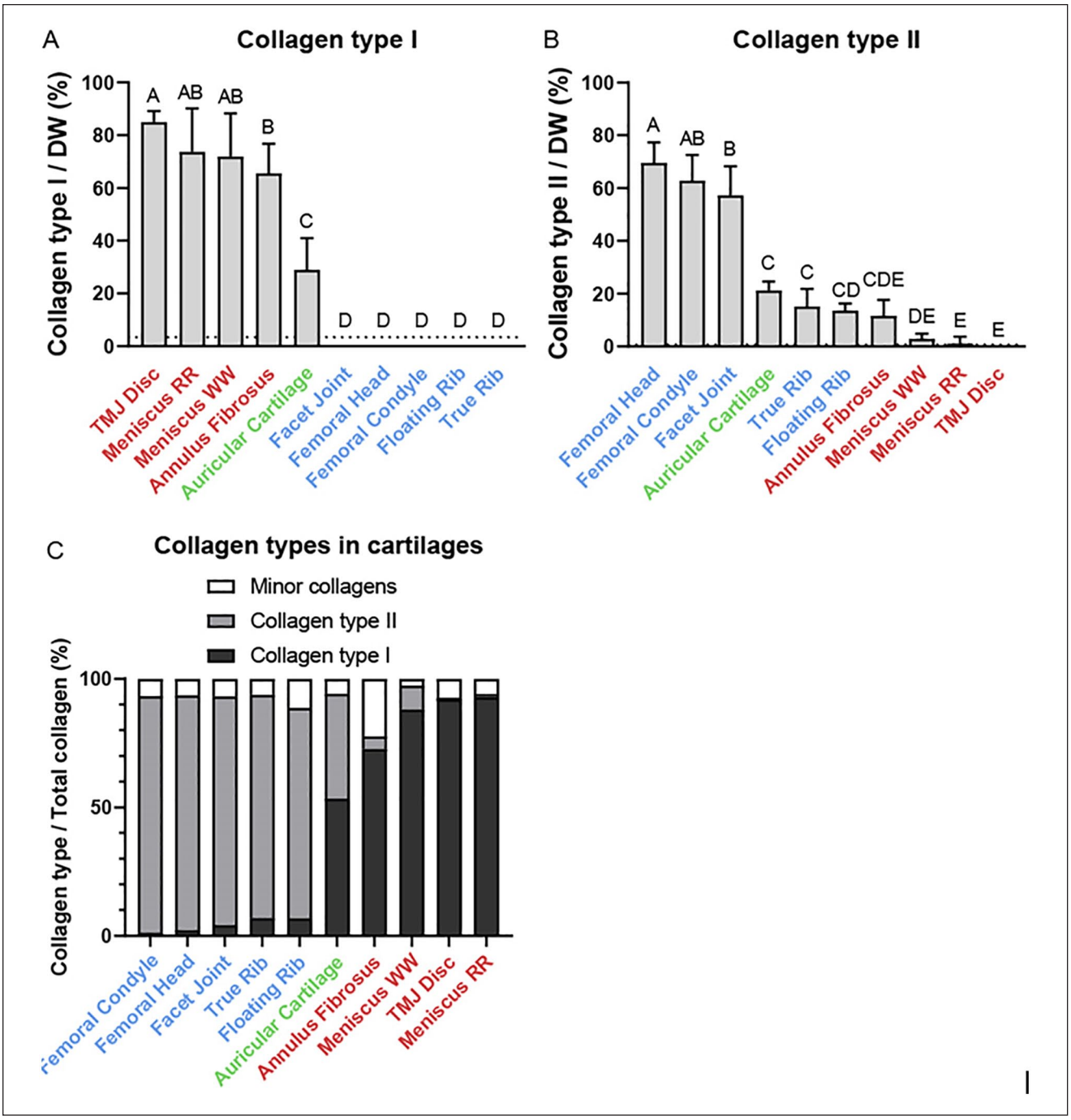

Figure 2. Collagen subtype quantification in the cartilages of the Yucatan minipig. (**A**) Collagen type I normalized to dry weight. (**B**) Collagen type II normalized to dry weight. Dashed lines: limits of quantification of the LC-MS/MS assay. (**C**) Bottom-up proteomics analysis of collagens. Hyaline, elastic, and fibrocartilage x-axis labels are marked with blue, green, and red colors, respectively. LC-MS = liquid chromatography-mass spectrometry; DW = dry weight; TMJ = temporomandibular joint; RR = red-red; WW = white-white.

floating rib, femoral condyle, femoral head, facet joint) had a quantity of collagen type I that was below the LOQ. The articular cartilages (femoral head, femoral condyle, facet joint) had the highest amount of collagen type II per DW (69.5% ± 7.8%, 62.8% ± 9.7%, 57.3% ± 11.1%, respectively); the femoral head cartilage had significantly ($P = 0.02$) higher collagen type II than facet joint cartilage. None of the fibrocartilages had significantly different amounts of collagen type II per DW, and in all TMJ disc samples, the amount of collagen type II was below the

LOQ. For the hyaline costal cartilages, collagen type II per DW was significantly lower than other hyaline cartilages; this is due to a high degree of calcification of rib cartilages in the skeletally mature pigs.

Cartilage Crosslinks

The mature (PYR) and immature (DHLNL) crosslink contents of the cartilages are depicted in **Figure 3**. Normalized to collagen as measured by hydroxyproline content, the highest PYR content was found in the auricular cartilage (62.0 ± 13.0 mmol/mol), while most fibrocartilages such as the red-red meniscus (19.6 ± 6.6 mmol/mol) had higher mean PYR than hyaline cartilage such as the femoral condyle (8.1 ± 2.2 mmol/mol). Normalized to collagen, there were no significant differences in DHLNL content among all cartilage types. Normalized to dry weight, all elastic and fibrocartilages except for annulus fibrosus have significantly more PYR than hyaline cartilages. For example, red-red meniscus has the highest PYR/DW at 2420 ± 568 ng/mg, whereas true rib cartilage has the lowest PYR/DW at 609 ± 381 ng/mg. A similar pattern was found with DHLNL normalized to dry weight, where most fibrocartilages had higher mean DHLNL/DW than hyaline cartilages, with annulus fibrosus being an exception. For example, TMJ disc (692 ± 163 ng/mg) had significantly more DHLNL/DW than true rib (242 ± 106 ng/mg), The "maturity ratio," defined as the molar ratio of PYR to DHLNL (**Fig. 3E**), was highest in the auricular cartilage (10.4 ± 2.3 mol/mol) and had a higher mean in all fibrocartilages than hyaline cartilages, but this difference was only significant for annulus fibrosus (4.0 ± 2.0 mol/mol).

Bottom-up Proteomics Analysis

A full list of relative proportions of all quantified proteins with greater than 0.1% protein per total protein can be found in **Table 2**. Collagen results are summarized in **Figure 2C**. In hyaline cartilages, collagen type II predominates over collagen type I, varying from a 12-fold difference (floating rib) to a 74-fold difference (femoral condyle). In auricular cartilage, collagen types I and II are very close, with about a 1.3-fold higher amount of collagen type I. This is consistent with a 1.4-fold higher amount of collagen type I in auricular cartilage, as found via high-throughput subtyping (**Fig. 1A and B**). All fibrocartilages have much higher collagen type I than type II, ranging from a 9.5-fold difference in the annulus fibrosus to a 157-fold difference in the red-red meniscus. In most cartilages, minor collagens (those aside from collagen types I and II) account for a small proportion of total collagen, ranging from 2.7% in the annulus fibrosus to 12.7% in the floating rib. The exception is the white-white meniscus which contained 28.8%, most of which comes from collagen type III; the white-white meniscus contained 24.7% of collagen type III per total collagen, the highest among any cartilages tested. The most prominent minor collagens were collagen types III, IX, XI, and XVI in hyaline cartilages and types III, V, VI, and XI in elastic and fibrocartilages. Other proteins that were found in the ECM include aggrecan core protein, hyaluronan and proteoglycan link protein 1, biglycan, cartilage intermediate layer protein 1, and decorin.

Histology

Histological stains on all cartilages are shown in **Figure 4**. H&E histology was used to visualize cells and ECM. Fibrocartilages, which stained more heavily with eosin than hyaline, and elastic cartilages showed striated patterns of anisotropic collagen organization. Histological results were consistent with the literature in terms of the morphology and relative staining intensities; for example, hyaline and elastic cartilages appeared more isotropic, with less strong eosin staining and stronger hematoxylin staining due to higher quantities of glycosaminoglycans (GAGs) in the tissues.[18] The true rib morphology had a fragmented appearance in areas of high calcification. PR staining, similar to H&E staining, stained more intensely for collagen in the fibrocartilages and appeared fibrous and anisotropic. PR staining intensity was lower in the nonfibrous cartilages, and there was less organization of collagen fibers.

Discussion

In this experiment, we developed and optimized 2 LC-MS assays for quantification of collagen subtypes and collagen crosslinks, and confirmed the hypotheses that LC-MS can be used as a sensitive, specific, quantification method for collagen subtypes and crosslinks in biological tissues. With the parameters detailed in **Table 1**, researchers with access to mass spectrometers can run these assays. The collagen subtyping assay has advantages over other collagen assays; it is specific to collagen subtype, can be run with a 5-minute chromatography gradient, and does not require expensive antibodies. The collagen crosslinks assay can simultaneously detect hydroxyproline and crosslinks (immature and mature) in a 10-minute gradient; this assay offers researchers an additional low-cost and low-operator-time technique to study biological tissues.

To demonstrate these novel tools, 10 different cartilages of the Yucatan minipig were analyzed with the collagen subtype and crosslink quantification assays. The collagen subtyping assay accurately showed a majority of collagen type I in fibrocartilages and a majority of collagen type II in hyaline cartilages, and the crosslinks assay showed that the collagen of hyaline cartilages contains more crosslinks than the collagen of fibrocartilages. A bottom-up proteomics analysis was also performed, and the proteomes, quantified in **Table 2**, will allow cartilage researchers and clinicians to

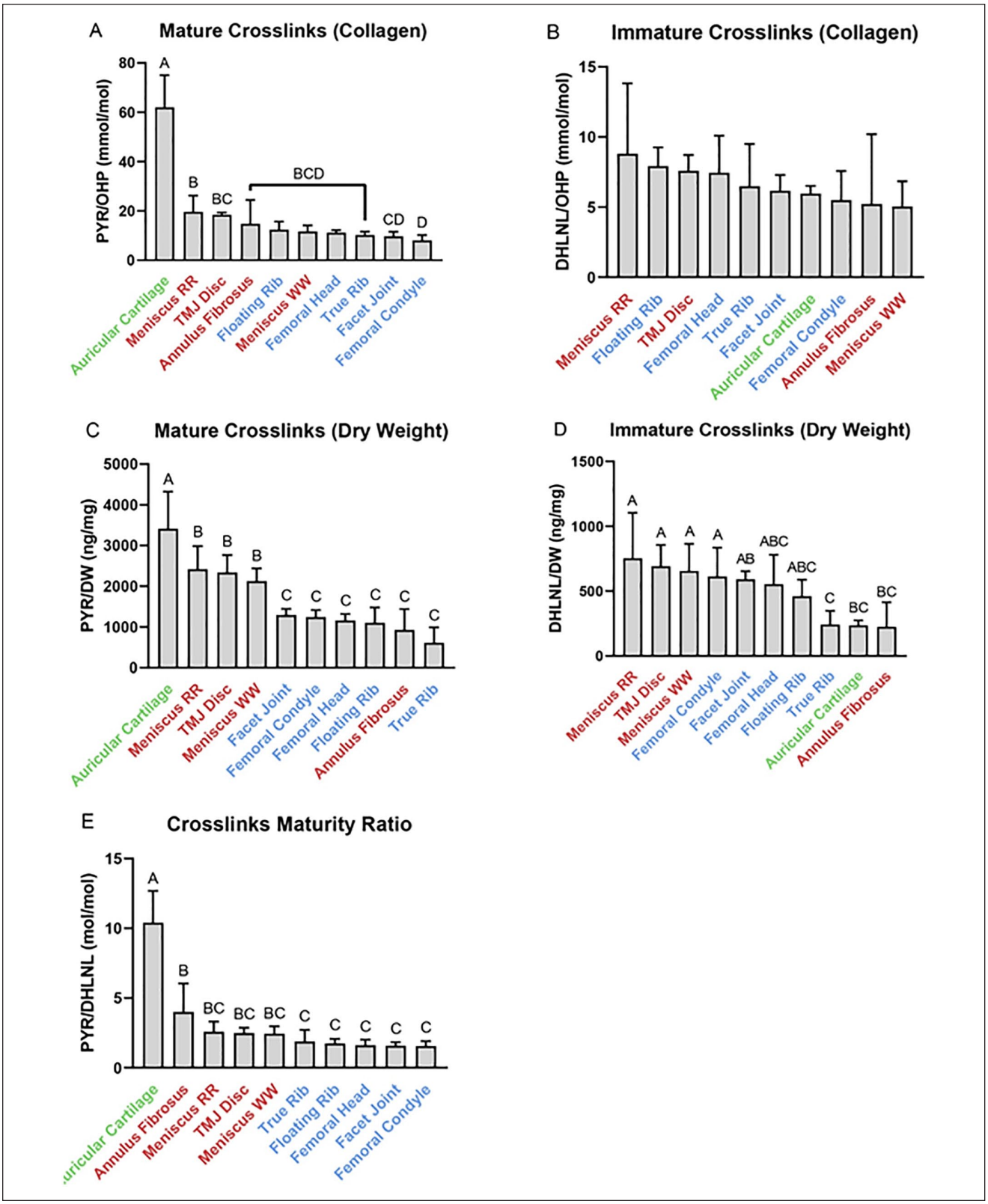

Figure 3. Crosslink quantification in the cartilages of the Yucatan minipig. (**A, C**) Mature crosslinks (PYR) normalized to hydroxyproline and dry weight, respectively. (**B, D**) Immature crosslinks (DHLNL) normalized to hydroxyproline and dry weight, respectively. (**E**) Maturity ratio, or the molar ratio of PYR to DHLNL. Hyaline, elastic, and fibrocartilage x-axis labels are marked with blue, green, and red colors, respectively. DHLNL = dihydroxylysinonorleucine; PYR = pyridinoline; OHP = hydroxyproline; TMJ = temporomandibular joint; DW = dry weight.

Table 2. Bottom-up Proteomics Results on Yucatan Minipig Cartilages.

		Protein/Total Protein									
Gene	Protein Name	FC	FH	FJ	TR	FR	AC	AF	MW	TD	MR
PGCA	Aggrecan core protein	0.15	0.21	0.18	0.00	0.45	0.04	0.02	0.03	0.00	0.00
PGS1	Biglycan	0.09	0.18	0.13	0.00	0.00	0.08	0.01	0.02	0.00	0.00
CILP1	Cartilage intermediate layer protein 1	0.13	0.14	0.12	0.00	0.00	0.00	0.02	0.06	0.00	0.00
COL1A1	Collagen type I alpha 1	1.11	2.17	3.65	6.34	6.38	34.45	60.01	50.71	63.71	61.32
COL1A2	Collagen type I alpha 2	0.11	0.08	0.51	0.46	0.31	18.08	27.58	21.46	28.53	30.17
COL2A1	Collagen type II alpha 1	91.06	89.87	87.20	84.60	80.90	40.14	9.21	4.81	1.15	0.58
COL3A1	Collagen type III alpha 1	4.42	3.21	3.36	0.32	0.02	3.84	1.56	19.68	4.19	5.76
COL4A1	Collagen type IV alpha 1	0.07	0.09	0.05	0.79	0.32	0.03	0.02	0.00	0.00	0.00
COL4A2	Collagen type IV alpha 2	0.02	0.01	0.01	0.30	0.26	0.01	0.00	0.00	0.00	0.00
COL4A3	Collagen type IV alpha 3	0.05	0.07	0.03	0.04	0.15	0.03	0.04	0.04	0.08	0.05
COL4A4	Collagen type IV alpha 4	0.00	0.00	0.00	0.00	0.00	0.01	0.01	0.01	0.10	0.02
COL4A5	Collagen type IV alpha 5	0.01	0.02	0.01	0.44	0.32	0.03	0.05	0.07	0.08	0.15
COL5A1	Collagen type V alpha 1	0.07	0.04	0.09	0.03	0.01	0.05	0.09	0.42	0.16	0.25
COL5A2	Collagen type V alpha 2	0.07	0.03	0.07	0.01	3.10	0.06	0.08	0.30	0.09	0.09
COL5A3	Collagen type V alpha 3	0.15	0.47	0.14	0.02	0.02	0.14	0.05	0.62	0.23	0.14
COL6A2	Collagen type VI alpha 2	0.06	0.09	0.08	0.01	0.01	0.16	0.05	0.10	0.04	0.05
COL6A3	Collagen type VI alpha 3	0.10	0.18	0.14	0.00	0.00	0.17	0.17	0.33	0.19	0.19
COL9A1	Collagen type IX alpha 1	0.21	0.26	0.37	0.88	0.76	0.00	0.00	0.00	0.02	0.06
COL9A2	Collagen type IX alpha 2	0.14	0.16	0.25	0.79	0.33	0.00	0.02	0.25	0.22	0.02
COL10A1	Collagen type X alpha 1	0.00	0.00	0.00	0.17	0.98	0.03	0.01	0.00	0.00	0.04
COL11A1	Collagen type XI alpha 1	0.40	0.43	0.73	1.15	1.61	0.47	0.23	0.11	0.07	0.10
COL11A2	Collagen type XI alpha 2	0.58	0.70	1.05	1.02	2.03	0.48	0.10	0.05	0.10	0.06
COL12A1	Collagen type XII alpha 1	0.04	0.22	0.13	0.01	0.00	0.07	0.06	0.03	0.07	0.08
COL15A1	Collagen type XV alpha 1	0.00	0.00	0.00	0.00	0.00	0.00	0.04	0.06	0.18	0.08
COL16A1	Collagen type XVI alpha 1	0.15	0.19	0.09	0.03	0.02	0.07	0.01	0.00	0.01	0.00
COL27A1	Collagen type XXVII alpha 1	0.05	0.09	0.06	0.07	0.28	0.04	0.07	0.08	0.08	0.19
COL28A1	Collagen type XXVIII alpha 1	0.00	0.00	0.00	0.00	0.89	0.00	0.00	0.00	0.00	0.00
CUBN	Cubilin	0.00	0.00	0.00	0.00	0.00	0.11	0.25	0.01	0.12	0.27
COX6C	Cytochrome c oxidase subunit 6C	0.00	0.00	0.00	0.17	0.14	0.00	0.00	0.00	0.00	0.00
PGS2	Decorin	0.16	0.11	0.14	0.09	0.11	0.11	0.07	0.10	0.10	0.05
FMOD	Fibromodulin	0.02	0.03	0.03	0.05	0.00	0.03	0.01	0.02	0.01	0.01
G3P	Glyceraldehyde-3-phosphate dehydrogenase	0.02	0.16	0.08	0.01	0.00	0.01	0.02	0.01	0.01	0.00
HBA	Hemoglobin subunit alpha	0.00	0.15	0.05	0.00	0.00	0.01	0.02	0.01	0.01	0.00
H4	Histone H4	0.04	0.04	0.08	0.03	0.02	0.05	0.01	0.01	0.01	0.02
HPLN1	Hyaluronan and proteoglycan link protein 1	0.10	0.14	0.30	0.13	0.11	0.16	0.03	0.04	0.00	0.01
MFGM	Lactadherin	0.07	0.13	0.23	0.08	0.10	0.10	0.02	0.08	0.00	0.00
MYG	Myoglobin	0.00	0.01	0.15	0.00	0.00	0.00	0.01	0.00	0.00	0.00
MYH7	Myosin-7	0.00	0.01	0.00	1.75	0.03	0.00	0.00	0.00	0.00	0.00
ROCK2	Rho-associated protein kinase 2	0.01	0.03	0.02	0.01	0.00	0.17	0.01	0.19	0.23	0.01
TENA	Tenascin	0.14	0.09	0.11	0.01	0.00	0.01	0.00	0.05	0.03	0.05
KSYK	Tyrosine-protein kinase SYK	0.03	0.01	0.04	0.03	0.14	0.02	0.00	0.00	0.05	0.03
VIME	Vimentin	0.02	0.02	0.02	0.00	0.03	0.57	0.00	0.00	0.01	0.02

Only proteins that comprise greater than 0.01% of total protein content are included.
FC = femoral condyle; FH = femoral head; FJ = facet joint cartilage; TR = true rib; FR = floating rib; AC = auricular (ear) cartilage; AF = annulus fibrosus; MW = meniscus white-white region; TD = temporomandibular joint disc; MR = meniscus red-red region.

better understand the matrix that comprises these tissues. With bottom-up proteomics analysis, evidence that hyaline and fibrous cartilages exist on a spectrum was supported by the quantification of the ratio of collagen types I and II. Notably, the fibrocartilage of the knee meniscus revealed regional differences between the white-white and red-red

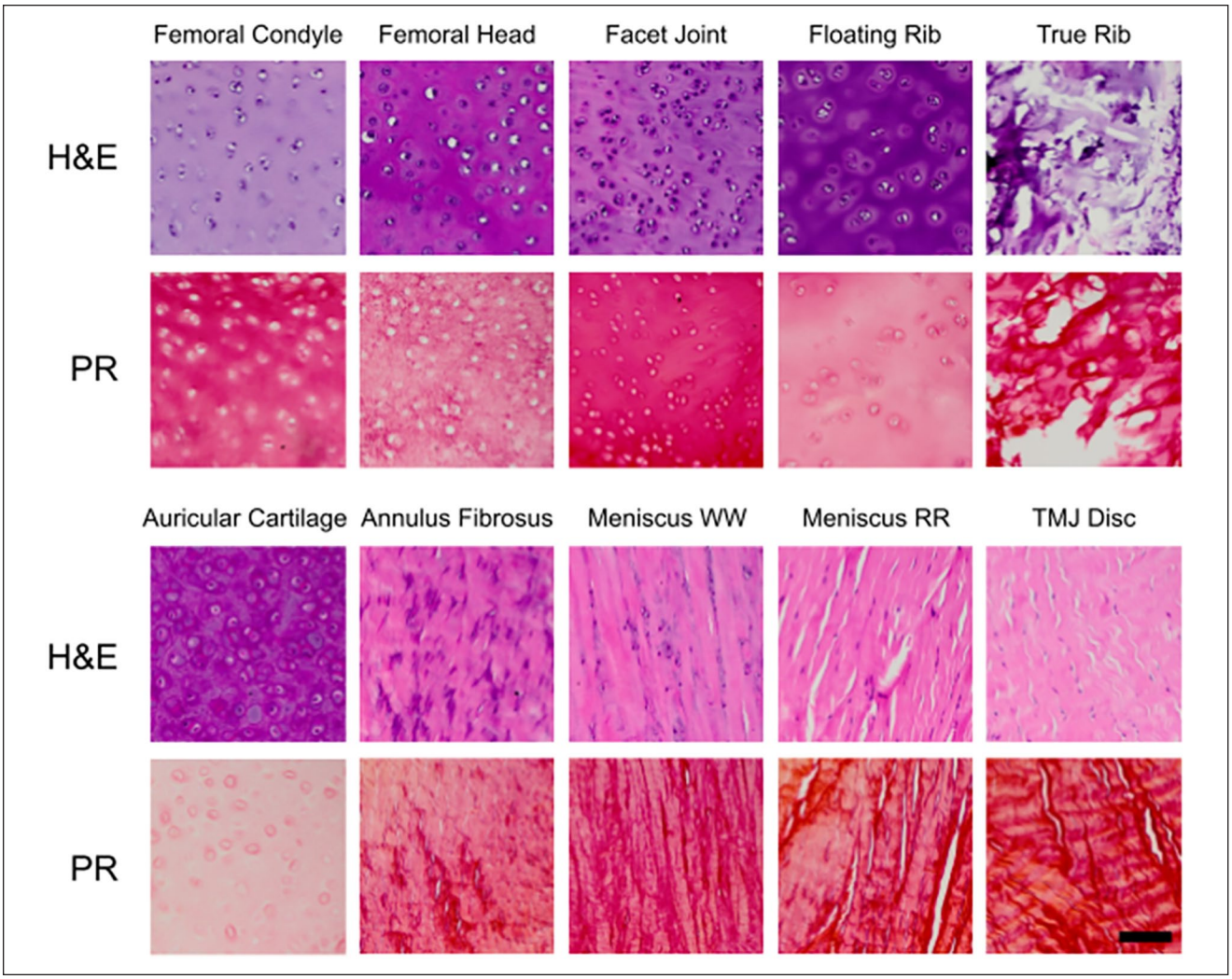

Figure 4. Histological stains on minipig cartilages. H&E, hematoxylin and eosin; PR, picrosirius red; TMJ = temporomandibular joint. Scale bar, 100 μm.

region, although this difference is substantially less than what has been reported in other work, as described below. Overall, this study provides (1) a basis for researchers to simultaneously quantify collagen types I and II in a high-throughput manner, (2) relative quantities of the 42 most abundant proteins found in 10 cartilages, and (3) evidence for a spectrum of native hyaline and fibrous cartilages.

Determining collagen content is a vital step for characterization of biological tissues and products. The currently practiced methods for collagen quantification are described in **Table 3**, which shows that the LC-MS/MS collagen subtype quantification technique developed in this work is more cost-effective and specific than other options; the novel subtyping assay is a fraction of the cost of ELISA or Orbitrap-based label-free quantification. While some previous work has been done toward developing MS assays for quantitative collagen subtyping,[19] the high-throughput method used in this study is faster (5-minute versus 60-minute chromatography), eliminates a lengthy salt cutting procedure, and uses a single-step high-temperature trypsin digestion rather than a combination of trypsin and highly toxic cyanogen bromide.[20] Although some cartilage types in this sample set yielded collagen readings below the LOQ (collagen type I in hyaline cartilages and collagen type II in TMJ disc), it is possible that these collagen types can be quantified with the same assay on a different instrument; more recent mass spectrometer models have been advertised to greatly improve the signal-to-noise ratio compared with older models, such as the one used in this study. With these newer models, the target peptide approach can be used to quantify minor collagen subtypes simultaneously with collagen types I and II in a high-throughput and low-cost manner. The work presented in this study is relevant to tissue engineers, who may use collagen content as a benchmark due its role in mechanical properties of tissues such as cartilages,[21] blood vessels,[22] ligaments,[5] and skin.[23]

Table 3. Comparison of Collagen Assays.

Method	Price (Approx.)[a]	Operator Time (h)[a]	Notes
Hydroxyproline assay	$50	6	Not specific to different types of collagen
ELISA	$500 (1 collagen type)	6	Antibodies for many minor collagen types unavailable
Label-free Orbitrap-based quantification	$4,000 (All collagen types)	2 (36-h machine time)	Low-throughput for large sample sets
Label-free LC-MS/MS with multiple reaction monitoring	$40 (targeted collagen types)	2 (3-h machine time)	Requires additional method development for minor collagens

LC-MS = liquid chromatography-mass spectrometry; ELISA = enzyme-linked immunosorbent assay.
[a]For 36 samples. Prices are estimated based on reagent costs and machine usage rates at the High-end Mass Spectrometry Facility and the Mass Spectrometry Facility at the University of California, Irvine.

Collagen quantification is important in other fields as well; collagen content has been correlated to malignancy of various cancers,[24] and it is used in many products in the cosmetics industry[25,26] and food and beverage industry.[27]

While collagen crosslink quantification assays have recently seen improvements in the development of silica hydride–based chromatography and mass spectrometry,[7] the assay in this study features an improvement in using a 10-minute chromatography gradient for a low assay runtime compared with commonly used crosslinks assays (30-45 minutes). This collagen crosslink assay, like the collagen subtype quantification assay, is applicable to collagenous tissues all over the body. A novel aspect of this work is the usage of a maturity ratio for cartilages. While other groups have looked at the ratio of immature and mature crosslinks in collagenous tissues,[6] this is the first study that compares this ratio across different types of cartilage. This study showed that fibrocartilages have a greater maturity ratio than hyaline cartilages. Whether or not this is due to rates of collagen turnover in these cartilages, mechanical demands of the tissue, or other factors is yet to be determined.

The bottom-up proteomics method in this study provided quantitative evidence that a spectrum of hyaline and fibrocartilages exists in the Yucatan minipig, shown in the ratio of collagen type I to collagen type II. In hyaline cartilage, the ratio of collagen type II to collagen type I varies from about 74:1 in femoral condyle to about 12:1 in floating rib. In fibrocartilage, the ratio of collagen type I to collagen type II ranges from over 150:1 in the red-red meniscus to less than 10:1 in the annulus fibrosus. Auricular cartilage, the only elastic cartilage in this data set, contains roughly the same amount of collagen types I and II. This wide array of ratios suggests the existence of a spectrum of fibrous and hyaline cartilage rather than discrete categories.

A spectrum of cartilage properties also appears not only in the collagen ratios but also in the collagen crosslinks. As shown in **Figure 3A and C**, fibrocartilages had greater quantities of mature crosslinks per hydroxyproline and dry weight than hyaline cartilages. It is possible that this may arise from the way that collagen type II crosslinks to collagen type XI in hyaline cartilage ECM,[28] given that the bottom-up proteomics revealed 0.99% to 3.6% collagen type XI per protein in the hyaline cartilages. Collagen type I can crosslink to collagen type V,[29] and collagen type V was less abundant, at 0.21% to 1.34% in the fibrocartilages, so it is possible that more crosslinks are formed between collagen types I and V than between II and XI. The difference in crosslinking may also arise from differences in the structure of the collagen molecules. One study has reported that a higher amount of glycosylated hydroxylysine residues in collagen type II results in a larger molecular spacing compared with collagen type I, allowing collagen type II to contain 50% to 100% more water than collagen type I, and this property may allow collagen type II to resist osmotic swelling from GAGs in cartilage ECM to dissipate compressive loading.[30] This increased spacing, which is needed for a collagen network that better resists osmotic swelling, may reduce the efficiency of collagen crosslink kinematics. Additional experiments will need to be performed to fully understand the differences in crosslinking between hyaline cartilages and fibrocartilages.

When damage to hyaline articular cartilage results in fibrocartilage formation, via bleeding either from subchondral bone or from microfracture procedures, a fibrocartilage repair tissue is formed in the defect that contains both collagen types I and II,[31] which fails mechanically in the long term.[32] The failure of this fibrocartilage repair tissue may be in part due to the aforementioned role of collagen II in dissipating compressive forces; if the ECM of the repair tissue is of the wrong composition, it may not stand up to the large, repeated forces withstood by hyaline articular cartilage. While current methods for repair of cartilage defects are unsuccessful in the long term, tissue engineering is a promising strategy to generate biomimetic cartilage implants for cartilage regeneration.[33]

Because different types of collagen are implicated in the loading capabilities of cartilage tissues, engineered cartilages must be designed to match the ECM of the cartilage that they

are designed to replace. The bottom-up proteomics analysis of the cartilages in this study can be used to define gold standard ratios of collagen types I and II in engineered cartilages. Tissue engineering studies using the self-assembling process have engineered a spectrum of fibrous and hyaline neocartilages by varying the time of 3-dimensional aggregate culture,[13] although collagen types I and II were not quantified. Other studies have used different ratios of cell sources (e.g., meniscus fibroblasts and articular chondrocytes) to achieve different ratios of collagen types.[34] Additional studies to fine-tune these techniques and generate specific collagen type I:II ratios must be completed to replace different cartilages around the body. While the minipig is a promising animal model for cartilage repair[8,9] and has been used in attempts at cartilage regeneration using tissue-engineered implants,[35] a thorough characterization on the hyaline-fibrocartilage spectrum of human cartilage must also be completed to determine engineering specifications for tissue-engineered cartilage in humans because interspecies differences in collagen content have been noted.[36] In addition, the Yucatan minipigs in this study were all skeletally mature. Because the collagen and crosslink content of cartilage changes with age and disease,[37,38] additional characterization of cartilages at different ages will be needed for a diverse patient population.

The relative proportion of collagen types I and II in the knee meniscus is supported by conflicting literature. An early study claimed that collagen of the porcine meniscus is completely type I,[39] but a subsequent study claimed that the white-white portion of the bovine meniscus is 60% collagen type II and 40% collagen type I.[14] This idea that the white-white meniscus contains abundant collagen type II, and, thus, is reminiscent of hyaline articular cartilage, has become accepted in the meniscus field.[33,40] A more recent proteomics analysis on various cartilages reveals over a 12-fold ratio of collagen type I to collagen type II in the human knee meniscus,[41] although the region was not specified. The bottom-up proteomics analysis in our study revealed a 15-fold ratio of collagen type I to type II in the white-white region and a greater than 150-fold ratio in the red-red region. While there is indeed a stark difference in this ratio between the 2 regions, these data, in conjunction with the histological staining (**Fig. 4**), suggest that the white-white meniscus of the Yucatan minipig is indeed a true fibrocartilage, with a substantially dissimilar ECM from hyaline cartilage. The white-white meniscus also had the highest amount of collagen type III out of any of the cartilages studied. To our knowledge, this is the first study that reports a high amount of collagen type III in the white-white meniscus. One study has shown that collagen type III is intensely expressed at the surfaces of the meniscus[42]; because the white-white region is exceedingly thin compared with the red-red region, the higher quantity of collagen type III could be a result of this high surface area to volume ratio. Another study has highlighted that collagen type III plays a crucial structural role in meniscus ECM by maintaining fibril spacing and diameter,[43] but did not quantify the amount of collagen type III in the tissue. Collagen type III comprises up to 20% of the protein in cartilages, suggesting that collagen type III should be considered a major collagen type, along with collagen types I and II. This finding warrants further investigation into the mechanical roles of collagen type III in cartilages. A study on human cartilages will be important to determine the ECM characteristics of the human meniscus, particularly the quantity of collagen types I, II, and III in different regions.

In this study, we developed LC-MS assays to quantify collagen subtypes and crosslinks in biological tissues. These assays are inexpensive, require a low operator time, and can be modified to quantify minor collagen types and their crosslinks. As a demonstration of these assays, they were applied to the cartilages of the Yucatan minipig, a promising animal model for cartilage repair. Collagen types I and II, along with the crosslinks PYR and DHLNL, were quantified in hyaline, elastic, and fibrocartilages. Bottom-up proteomics revealed a spectrum of collagen ratios in these tissues, thus showing the existence of a hyaline-fibrocartilage spectrum in native cartilage. This is one of many potential ways that the high-throughput collagen subtyping developed in this work can be used for characterization of collagenous tissues, informing best practices for tissue engineers and surgeons as they develop treatment strategies.

Acknowledgments and Funding

The authors would like to acknowledge Benjamin Katz and Felix Grun at the UCI Mass Spectrometry Facility for guidance on the collagen subtype and crosslink LC-MS quantification methods. The authors would like to acknowledge Clinton Yu at the UCI High-end Mass Spectrometry Facility for running samples on the Orbitrap mass spectrometer and assistance with database searching and MaxQuant analysis. The author(s) disclosed receipt of the following financial support for the research, authorship, and/or publication of this article: This work was funded by NIH grant nos. R01DE015038, R01AR071457, and R01AR067821.

Declaration of Conflicting Interests

The author(s) declared the following potential conflicts of interest with respect to the research, authorship, and/or publication of this article: Kyriacos A. Athanasiou and Jerry C. Hu are scientific consultants at Cartilage Inc.

Ethical Approval

Ethical approval was not sought for this study because the tissue samples used in this study were excised from pigs that were previously culled for purposes unrelated to this work.

Availability of Data

The proteomics data have been deposited to the ProteomeXchange Consortium via the PRIDE partner repository with the data set

identifier PXD025482. The data sets used and/or analyzed during the current study are available from the corresponding author on reasonable request.

ORCID iD

Kyriacos A. Athanasiou https://orcid.org/0000-0001-5387-8405

References

1. Bielajew BJ, Hu JC, Athanasiou KA. Collagen: quantification, biomechanics and role of minor subtypes in cartilage. Nat Rev Mater. 2020;5:730-47. doi:10.1038/s41578-020-0213-1.
2. Ricard-Blum S, Ruggiero F. The collagen superfamily: from the extracellular matrix to the cell membrane. Pathol Biol. 2005;53:430-42.
3. Cissell DD, Link JM, Hu JC, Athanasiou KA. A modified hydroxyproline assay based on hydrochloric acid in Ehrlich's solution accurately measures tissue collagen content. Tissue Eng Part C Methods. 2017;23:243-50.
4. Yocum AK, Chinnaiyan AM. Current affairs in quantitative targeted proteomics: multiple reaction monitoring-mass spectrometry. Brief Funct Genomic Proteomic. 2009;8:145-57.
5. Eleswarapu SV, Responte DJ, Athanasiou KA. Tensile properties, collagen content, and crosslinks in connective tissues of the immature knee joint. PLoS ONE. 2011;6:e26178.
6. Yoshida K, Jiang H, Kim M, Vink J, Cremers S, Paik D, *et al*. Quantitative evaluation of collagen crosslinks and corresponding tensile mechanical properties in mouse cervical tissue during normal pregnancy. PLoS ONE. 2014;9:e112391.
7. Naffa R, Watanabe S, Zhang W, Maidment C, Singh P, Chamber P, *et al*. Rapid analysis of pyridinoline and deoxypyridinoline in biological samples by liquid chromatography with mass spectrometry and a silica hydride column. J Sep Sci. 2019;42:1482-8.
8. Goetz JE, Fredericks D, Petersen E, Rudert MJ, Baer T, Swanson E, *et al*. A clinically realistic large animal model of intra-articular fracture that progresses to post-traumatic osteoarthritis. Osteoarthritis Cartilage. 2015;23:1797-805.
9. Vapniarsky N, Aryaei A, Arzi B, Hatcher DC, Hu JC, Athanasiou KA. The Yucatan minipig temporomandibular joint disc structure-function relationships support its suitability for human comparative studies. Tissue Eng Part C Methods. 2017;23:700-9.
10. Sophia Fox AJ, Bedi A, Rodeo SA. The basic science of articular cartilage: structure, composition, and function. Sports Health. 2009;1:461-8.
11. Eyre DR, Wu JJ. Collagen of fibrocartilage: a distinctive molecular phenotype in bovine meniscus. FEBS Lett. 1983; 158:265-70.
12. Madsen K, von der Mark K, van Menxel M, Friberg U. Analysis of collagen types synthesized by rabbit ear cartilage chondrocytes in vivo and in vitro. Biochem J. 1984; 221:189-96.
13. Murphy MK, Masters TE, Hu JC, Athanasiou KA. Engineering a fibrocartilage spectrum through modulation of aggregate redifferentiation. Cell Transplant. 2015;24:235-45.
14. Cheung HS. Distribution of type I, II, III and V in the pepsin solubilized collagens in bovine menisci. Connect Tissue Res. 1987;16:343-56.
15. Qeli E, Omasits U, Goetze S, Stekhoven DJ, Frey JE, Basler K, *et al*. Improved prediction of peptide detectability for targeted proteomics using a rank-based algorithm and organism-specific data. J Proteomics. 2014;108:269-83.
16. Cox J, Mann M. MaxQuant enables high peptide identification rates, individualized p.p.b.-range mass accuracies and proteome-wide protein quantification. Nat Biotechnol. 2008;26:1367-72.
17. Brown WE, Huey DJ, Hu JC, Athanasiou KA. Functional self-assembled neocartilage as part of a biphasic osteochondral construct. PLoS ONE. 2018;13:e0195261.
18. Chiu L, Waldman S. Nanomaterials for cartilage tissue engineering. In: Nanomaterials and regenerative medicine. (y. Lin and T. Gong, eds), IAPC Publishing; Zagreb, Croatia, 2016, p. 417-51.
19. Pataridis S, Eckhardt A, Mikulikova K, Sedlakova P, Miksik I. Determination and quantification of collagen types in tissues using HPLC-MS/MS. Curr Anal Chem. 2009;5:316-23.
20. PubChem. Cyanogen bromide. Date unknown. Available from: https://pubchem.ncbi.nlm.nih.gov/compound/10476.
21. Haudenschild AK, Sherlock BE, Zhou X, Hu JC, Leach JK, Marcu L, *et al*. Nondestructive fluorescence lifetime imaging and time-resolved fluorescence spectroscopy detect cartilage matrix depletion and correlate with mechanical properties. Eur Cell Mater. 2018;36:30-43.
22. Latimer CA, Nelson M, Moore CM, Martin KE. Effect of collagen and elastin content on the burst pressure of human blood vessel seals formed with a bipolar tissue sealing system. J Surg Res. 2014;186:73-80.
23. Oxlund H, Andreassen TT. The roles of hyaluronic acid, collagen and elastin in the mechanical properties of connective tissues. J Anat. 1980;131:611-20.
24. Fang M, Yuan J, Peng C, Li Y. Collagen as a double-edged sword in tumor progression. Tumour Biol. 2014;35:2871-82.
25. De Boulle K, Swinberghe S, Engman M, Shoshani D. Lip augmentation and contour correction with a ribose cross-linked collagen dermal filler. J Drugs Dermatol. 2009;8:1-8.
26. Avila Rodríguez MI, Rodríguez Barroso LG, Sánchez ML. Collagen: a review on its sources and potential cosmetic applications. J Cosmet Dermatol. 2018;17:20-6.
27. León-López A, Morales-Peñaloza A, Martínez-Juárez VM, Vargas-Torres A, Zeugolis DI, Aguirre-Álvarez G. Hydrolyzed collagen—sources and applications. Molecules. 2019;24:4031.
28. Wu JJ, Eyre DR. Structural analysis of cross-linking domains in cartilage type XI collagen. Insights on polymeric assembly. J Biol Chem. 1995;270:18865-70.
29. Niyibizi C, Eyre DR. Structural characteristics of cross-linking sites in type V collagen of bone. Chain specificities and heterotypic links to type I collagen. Eur J Biochem. 1994;224:943-50.
30. Grynpas MD, Eyre DR, Kirschner DA. Collagen type II differs from type I in native molecular packing. Biochim Biophys Acta. 1980;626:346-55.

31. Armiento AR, Alini M, Stoddart MJ. Articular fibrocartilage: why does hyaline cartilage fail to repair? Adv Drug Deliv Rev. 2019;146:289-305.
32. Solheim E, Hegna J, Inderhaug E. Long-term survival after microfracture and mosaicplasty for knee articular cartilage repair: a comparative study between two treatments cohorts. Cartilage. 2020;11:71-6.
33. Kwon H, Brown WE, Lee CA, Wang D, Paschos N, Hu JC, *et al*. Surgical and tissue engineering strategies for articular cartilage and meniscus repair. Nat Rev Rheumatol. 2019;15:550-70.
34. Aufderheide AC, Athanasiou KA. Assessment of a bovine co-culture, scaffold-free method for growing meniscus-shaped constructs. Tissue Eng. 2007;13:2195-205.
35. Vapniarsky N, Huwe LW, Arzi B, Houghton MK, Wong ME, Wilson JW, *et al*. Tissue engineering toward temporomandibular joint disc regeneration. Sci Transl Med. 2018; 10:eaaq1802.
36. Chiu LLY, Giardini-Rosa R, Weber JF, Cushing SL, Waldman SD. Comparisons of auricular cartilage tissues from different species. Ann Otol Rhinol Laryngol. 2017;126:819-28.
37. Lu W, Ding Z, Liu F, Shan W, Cheng C, Xu J, *et al*. Dopamine delays articular cartilage degradation in osteoarthritis by negative regulation of the NF-κB and JAK2/STAT3 signaling pathways. Biomed Pharmacother. 2019;119:109419.
38. Li Y, Wei X, Zhou J, Wei L. The age-related changes in cartilage and osteoarthritis. Biomed Res Int. 2013;2013:916530.
39. Eyre DR, Muir H. The distribution of different molecular species of collagen in fibrous, elastic and hyaline cartilages of the pig. Biochem J. 1975;151:595-602.
40. Makris EA, Hadidi P, Athanasiou KA. The knee meniscus: structure-function, pathophysiology, current repair techniques, and prospects for regeneration. Biomaterials. 2011;32: 7411-31.
41. Önnerfjord P, Khabut A, Reinholt FP, Svensson O, Heinegård D. Quantitative proteomic analysis of eight cartilaginous tissues reveals characteristic differences as well as similarities between subgroups. J Biol Chem. 2012;287:18913-24.
42. Mine T, Ihara K, Kawamura H, Date R, Umehara K. Collagen expression in various degenerative meniscal changes: an immunohistological study. J Orthop Surg. 2013;21:216-20.
43. Wang C, Brisson BK, Terajima M, Li Q, Hoxha K, Han B, *et al*. Type III collagen is a key regulator of the collagen fibrillar structure and biomechanics of articular cartilage and meniscus. Matrix Biol. 2020;85-86:47-67.